A coupled methodology for wave body interactions at the scale of a farm of wave energy converters including irregular bathymetry

Charrayre François, Christophe Peyrard, Michel Benoit, Aurélien Babarit

Proceedings of the ASME 2014 33rd International Conference on Ocean, Offshore and Arctic Engineering
OMAE2014
June 8-13, 2014, San Francisco, California, USA

OMAE2014-23457

A COUPLED METHODOLOGY FOR WAVE-BODY INTERACTIONS AT THE SCALE OF A FARM OF WAVE ENERGY CONVERTERS INCLUDING IRREGULAR BATHYMETRY

François Charrayre
Saint-Venant Hydraulics Laboratory
(EDF, CEREMA, Ecole des Ponts ParisTech)
6 quai Watier, 78400 Chatou, France
francois-externe.charrayre@edf.fr

Christophe Peyrard
Saint-Venant Hydraulics Laboratory
(EDF, CEREMA, Ecole des Ponts ParisTech)
6 quai Watier, 78400 Chatou, France
christophe.peyrard@edf.fr

Michel Benoit
Saint-Venant Hydraulics Laboratory
(EDF, CEREMA, Ecole des Ponts ParisTech)
6 quai Watier, 78400 Chatou, France
michel.benoit@edf.fr

Aurélien Babarit
LUNAM Université, École Centrale de Nantes - CNRS
1 rue de la Noe, 44300 Nantes France
aurelien.babarit@ec-nantes.fr

ABSTRACT

Knowledge of the wave perturbation caused by an array of Wave Energy Converters (WEC) is of great concern, in particular for estimating the interaction effects between the various WECs and determining the modification of the wave field at the scale of the array, as well as possible influence on the hydrodynamic conditions in the surroundings. A better knowledge of these interactions will also allow a more efficient layout for future WEC farms. The present work focuses on the interactions of waves with several WECs in an array. Within linear wave theory and in frequency domain, we propose a methodology based on the use of a BEM (Boundary Element Method) model (namely Aquaplus) to solve the radiation-diffraction problem locally around each WEC, and to combine it with a model based on the mild slope equation at the scale of the array. The latter model (ARTEMIS software) solves the Berkhoff's equation in 2DH domains (2 dimensional code with a z-dependence), considering irregular bathymetries. In fact, the Kochin function (a far field approximation) is used to propagate the perturbations computed by Aquaplus into Artemis, which is well adapted for a circular wave representing the perturbation of an oscillating body. This approximation implies that the method is only suitable for well separated devices. A main advantage of this coupling technique is that Artemis can deal with variable bathymetry. It is important when the wave farm is in shallow water or in nearshore areas. The methodology used for coupling the two models, with the underlying assumptions is detailed first. Validations test-cases are then carried out with simple bodies (namely heaving vertical cylinders) to assess the accuracy and efficiency of the coupling scheme. These tests also allow to analyze and to quantify the magnitude of the interactions between the WECs inside the array.
Keywords: wave energy converter, wave-body interaction, shallow water, Kochin function, far field approximation

NOMENCLATURE

ϕ velocity potential ($m^2.s^{-1}$)
ω pulsation ($rad.s^{-1}$)
G Green function
η free surface elevation (m)
g gravity ($m.s^{-2}$)
C velocity ($m.s^{-1}$)
k wave number (m^{-1})
H(θ) Kochin function
λ wave length (m)
M inertia matrix ($N.m^{-1}.s^2$)
K & Ka stiffness matrix ($N.m^{-1}$)
B & Ba damping matrix ($N.m^{-1}.s$)
Φ_D, Φ_{inc}, Φ_{Scat} diffracted, incident, scattered potential

INTRODUCTION

Today, wave energy takes an important place in ocean engineering research. Wave Energy Converters (WECs) are likely to be deployed in arrays of many devices, which raise particular issues and concerns in comparison with oil and gas or naval applications. Indeed, large wave farms may have a significant impact on the environment by altering the local wave climate with possible consequences on coastal processes. Some physical experiments may be conducted to study this effect (as in the Hydralab IV campaign [1] for instance), but they are challenging due to the finite extent of wave tanks. Thus, numerical experiments are favorized for cost and flexibility reasons.

Concerning the radiation/diffraction problem for oscillating WEC, studies can be based on previous works in electromagnetism or in the offshore field about diffraction around fixed (and then moving) bodies. Thus, the work of Twersky (1952) [2] on the diffraction of electromagnetic waves on parallel cylinders has been much exploited. Ohkusu (1974) [3] improved his technique of "multiple scattering" to apply it to fixed cylinders in water (offshore platform, bridges, ...). Then, from this idea, Spring and Monkmeyer (1974) [4] and Simon (1982) [5] developped a matrix method that Kagemoto and Yue (1985) [6] used to provide an exact algebraic method.

However, to date all the various numerical approaches (BEM, wave propagation models) suffer from theoretical and/or practical limitations [7]. To overcome these limitations, it has been proposed to couple the BEM method in the vicinity of the body with wave propagation models using domain decomposition [8]. The coupling of BEM (Boundary Element Method) with a phase resolving wave propagation model is further investigated in this paper. It is partly based on the multiple scattering method (previously reported). BEM is used to solve the radiation/diffraction problem of each WEC, and the wave model is used to propagate the different waves across the global domain. A far field approximation (Kochin function) is used to link these two codes. The use of the wave model allows taking into account a variable bathymetry. Thus it will be possible to understand its importance in the assessment of impact of wave farms on the local wave climate.

1 Approach and hypothesis

1.1 Global approach

In this section we will present a quick and efficient method to model the interactions between WECs. We work within the linear theory framework, which allows to decompose the wave field into a sum of potentials: incident and scattered (diffracted + radiated). We neglect the non linear interactions.

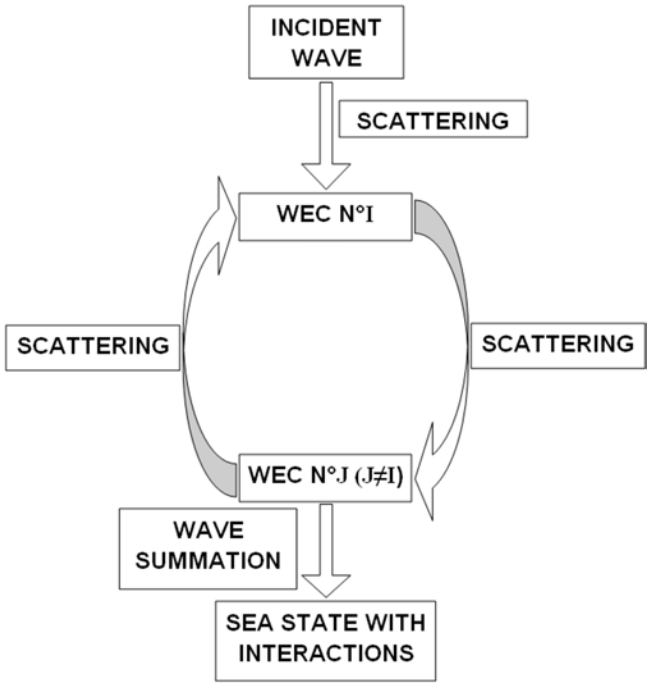

FIGURE 1: GLOBAL APPROACH

We work in the frequency domain. Our general approach is the following:

- Computation of the scatted potential with a BEM code. The Kochin function is obtained from the scattered potential. It depends only on the frequency and the local depth (and the wave direction if the WEC is not axisymmetric).
- Propagation of these disturbed potentials in the mild slope equation for each WEC a first time considering that the bodies are only affected by the global incident wave.

_ Propagation of the different disturbed waves which are the reactions of the bodies due to the other bodies perturbations.
_ Add these different disturbed potentials and the incident potential to get the total potential.

1.2 Scattering computing using linear potential flow model

To solve the radiation and diffraction problem, we choose to use a diffraction/radiation code based on the linear potential flow hypothesis.

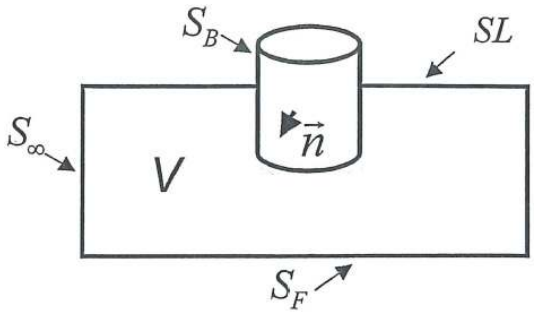

FIGURE 2: DIFFERENT PARTS OF THE DOMAIN

This type of code as Wamit [9] or Aquaplus [10] [11] is a BEM-3D code and meshes only the body wettered boundary. The hypotheses are:

_ flat bottom
_ linear theory (small wave height and small body motions)
_ the flow is irrotational
_ the fluid is inviscid and incompressible
_ the body has a mass homogeneously distributed

It solves the scattering problem for one body with appropriate boundary conditions:

_ fluid continuity in the fluid domain

$$\Delta\Phi = 0$$

_ kinematic free surface condition

$$\frac{\partial \eta}{\partial t} + \overrightarrow{\nabla}\eta.\overrightarrow{\nabla}\Phi = 0 \text{ if } M \in SL$$

_ dynamic free surface condition

$$\frac{\partial \Phi}{\partial t} + g\eta = 0 \text{ if } M \in SL$$

_ slip condition at the sea bottom

$$\frac{\partial \Phi}{\partial n} = 0 \text{ if } M \in S_F$$

_ body condition

$$\frac{\partial \Phi}{\partial n} = \overrightarrow{\nabla}\Phi.\overrightarrow{n} = \overrightarrow{V}.\overrightarrow{n} \text{ if } M \in S_B$$

_ scattering condition

$$\lim_{R\to\infty} \Phi_{Scat} = 0 \text{ with } R^2 = (x^2+y^2) \in S_\infty$$

To solve the scattering problem, Aquaplus considers 7 different problems, one for the diffraction problem and six for the radiation problems (one for each mode of motion), which can be added in the linear theory. The diffraction is computed considering the body is fixed in the incident field. The boundary conditions assume that:

$$\left(\frac{\partial \Phi_D}{\partial n}\right)_{S_B} = -\left(\frac{\partial \Phi_{inc}}{\partial n}\right)_{S_B} \tag{1}$$

which allows to obtain the diffracted potential.

To solve each of the six radiation problems, we consider that the body has a forced motion in a calm area (without waves). Each one is the solution of this equation:

$$\frac{\partial \Phi}{\partial n} = V_i.n_i \text{ with } M \in S_B \text{ and } i \in [1;6].$$

After the resolution of these problems, we add the seven potential which form the disturbed potential. This last one is then transmitted to the code which adds the different waves and propagates them. In fact, with a WEC in water, we have a potential of the form $\phi = \phi_i + \phi_p$ which is the superposition of the incident and disturbed potential. Aquaplus calculates this disturbed potential, which is a solution of equation (2)

$$\Omega(M)\,\phi_p(M) = \iint_{\overline{S_B}} \phi_P(M') \frac{\partial G(M,M')}{\partial n'} - \frac{\partial \phi_p(M')}{\partial n'} G(M,M') dS \tag{2}$$

with G the Green function and $\overline{S_B}$ the wetted boundary of the body.

The final equation of motion of each WEC solved by Aquaplus is:

$$M\,\ddot{X}(t) + (B+B_a)\,\dot{X}(t) + (K+K_a)X(t) = F(t) \tag{3}$$

A linear PTO (Power Take Off) is applied to each WEC by adding the additional damping and stiffness coefficients, respectively termed B_a and K_a.

1.3 Wave propagation using the mild slope equation

To propagate these different incident and scattered monochromatic waves in the domain of interest, we use the finite element code Artemis [12] which solves the mild slope equation and can take into account variable bathymetry. This code is an open source 2DH (2 dimensional code with a z-dependence) code that offers computational efficiency and accuracy.
With the previous hypothesis and the following analytical depth dependence for the potential,

$$\Phi(x,y,z,t) = \frac{cosh(k(z+h))}{cosh(kh)}.\phi(x,y).e^{i(k.x-\omega t)} \tag{4}$$

the reduced potential $\phi(x,y)$ is solution of the mild-slope equation derived by Berkhoff [13]:

$$\nabla.(CC_g\nabla\phi) + CC_gk^2\phi = 0 \tag{5}$$

with $C = \frac{\omega}{k}$ the phase velocity, $Cg = \frac{1}{2}\left[1+\frac{2kh}{sinh(2kh)}\right]$ the group velocity and k the wave number.
This equation is well adapted for a slowly changing bathymetry, but for rapidly varying bathymetry and dissipative processes (like waves breaking), it is necessary to add new terms:

$$\nabla.(CC_g\nabla\phi) + CC_gk^2\phi \underbrace{(1+f)}_{\text{bathymetry}} + \underbrace{ik\mu CC_g\phi}_{\text{dissipation}} = 0 \tag{6}$$

with:

$$f = \begin{cases} E_1(kh).(\nabla h)^2 + \frac{E_2(kh)}{k_o}.\Delta h & \text{rapidly varying bathymetry} \\ 0 & \text{slowly varying bathymetry} \end{cases} \tag{7}$$

where E_1 and E_2 are given by Chamberlain and Porter [14].
As in the present paper we have a small bottom slope, we use $f = 0$
As the Kochin function, a far-field approximation, is accurate beyond one wave length, we do not apply the scattered potential at the WEC boundary, but at the boundary of a fictitious island whose radius is chosen as half of the wave length.

2 Coupling between the two codes

2.1 Kochin function

A way to transmit information between the two codes is the use of the Kochin function. As it is a far field approximation, the different bodies will be spaced with a sufficient distance to compute realistic perturbation from each body. Typically, in the present paper, a distance of one wave length is necessary between two bodies.
First, we compute the Kochin function from the Aquaplus calculation:

$$H(\theta) = \iint_S \left(\frac{\partial\tilde{\phi}}{\partial n} - \tilde{\phi}_p\frac{\partial}{\partial n}\right) f_0(z')e^{ik(x'cos(\theta-\beta)+y'sin(\theta-\beta))}dS' \tag{8}$$

This function has been described in [8] based on [15]. From this angular function, we can provide the potential at the WEC boundary of the fictitious island around the WEC in Artemis. We can recompose the potential [16] [17]:

$$\phi_{Scat} = \sqrt{\frac{2}{\pi kR}}f_0(z).H(\theta).e^{i\left(kr-\frac{\pi}{4}\right)} + O\left(R^{-1}\right) \tag{9}$$

with $f_0(z) = -i\frac{Ag}{\omega}.\frac{cosh(k(z+h))}{cosh(kh)}$
As said previously, Aquaplus solves the scattering problem under the hypothesis of a flat bottom. It follows that for an axisymmetric body one calculation is enough whatever the incoming wave direction. For a farm of axisymmetric WECs, we thus need only one calculation per depth and wave frequency.

2.2 Validation

In the following, for the presented simulations, we use an incident wave of 2 m height ($\eta(t) = cos(\omega t)$) and 8 s period. The body is a truncated vertical cylinder of circular cross-section of 10 m draught and 10 m diameter (see next section).
In [8], the scattered wave computed by Aquaplus and the Kochin far field approximation are compared. This Kochin function is obtained by a specific calculation implemented in the Aquaplus code. After one wave length, the difference between these two results is lower than 1%. These results permit us to validate the Kochin function used to transmit informations about the scattered potential from Aquaplus to Artemis. To validate the use of the Kochin function in our coupled model, we compare the results obtained by propagation of the scattered wave with Artemis and the analytic value of this function. This comparison is made with a flat bottom. We use a cylindrical body which can only oscillate vertically. The angular Kochin function obtained with Aquaplus is plotted on fig.3

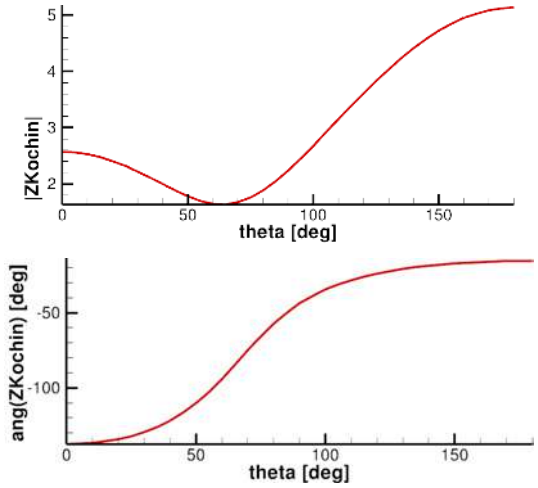

FIGURE 3: AMPLITUDE (TOP) AND ANGLE (DOWN) OF THE KOCHIN FUNCTION

This result is plotted only on a half of the circle because of the symmetry (the body is axi-symmetric, and the domain is infinite with a flat bottom).
Now we compare the analytical form with an Artemis result obtained with the Kochin function imposed on the inner boundary (figure 4). We use a disk-shaped area with an inner radius of 50 m (1/2 wavelength) and an outer radius of 280 m (∼3 wavelengths).

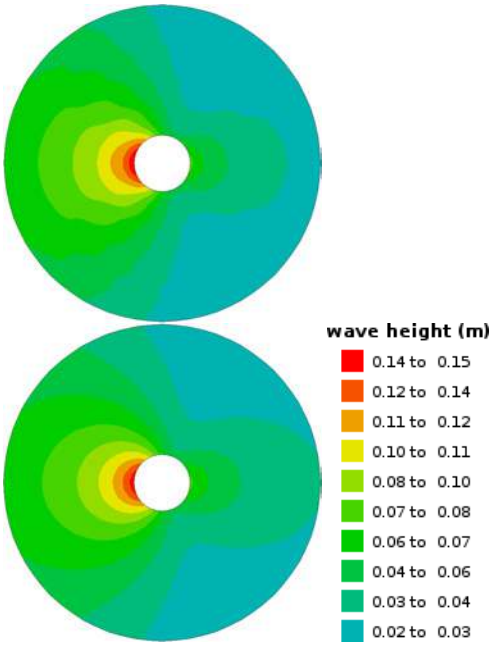

FIGURE 4: RADIATED WAVE HEIGHT. NUMERICAL (TOP) AND ANALYTICAL (BOTTOM) CALCULATION

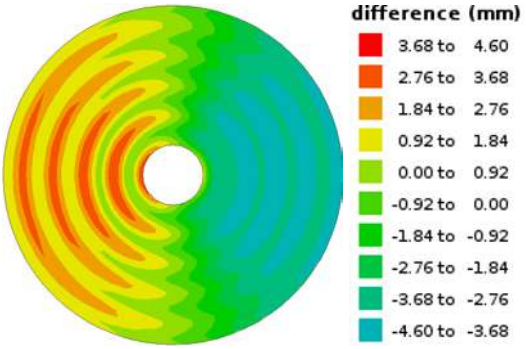

FIGURE 5: DIFFERENCE BETWEEN THE TWO RESULTS SHOWN FIG.4

These two results are very similar, and as shown on fig 5, the difference is very low (<3% surrounding the WEC, and lower in the far field). We can affirm that our model is able to propagate the perturbation potential given by the Kochin far field approximation. This good result allows us to add a variable bathymetry in the model.

3 Numerical computations

3.1 Presentation of the case

We present here only one case with a monochromatic incident wave of 8 s period and 1 m amplitude, but it is possible to work with a multidirectional and irregular wave train, as a superposition of many monochromatic and monodirectional waves.
The numerical domain is 60x20 wavelengths. The incident wave propagates from the left to the domain.

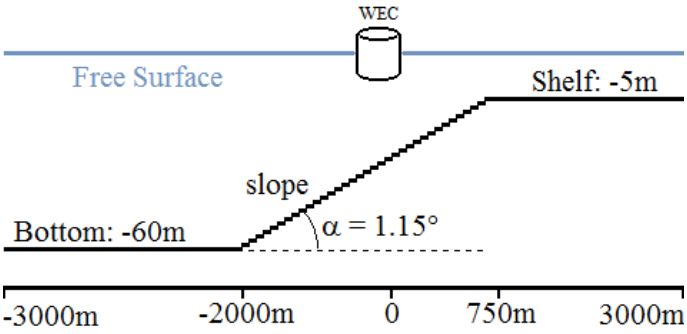

FIGURE 6: DOMAIN

The selected WEC is the same as used in the previous section: a truncated vertical cylinder of circular cross-section of 10

m draught and 10 m diameter.

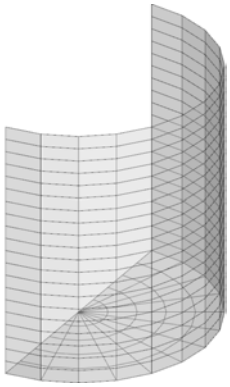

FIGURE 7: WEC VIEW

The WEC is constrained to move only vertically, following the z-axis. For a given incident wave (and a given damping and stiffness), the amplitude of its heave motion depends on the depth. For exemple, for the previously defined incident wave, with the flat bottom at 60m depth, the vertical motion is 10cm smaller than with the variable bathymetry (and the WECs at 20-25m depth).

3.2 Results for one WEC

First, we study a simple case with only one WEC. The advantage of this case is its simplicity because there is no interaction between different floating structures.
We compare the case with a variable bathymetry with the flat bathymetry case. The variable bathymetry has a constant slope of 1.15^o from 60 to 5 meter depth. The WEC is at a 20 m depth location. With the flat bottom, the depth is uniformly 60 m.

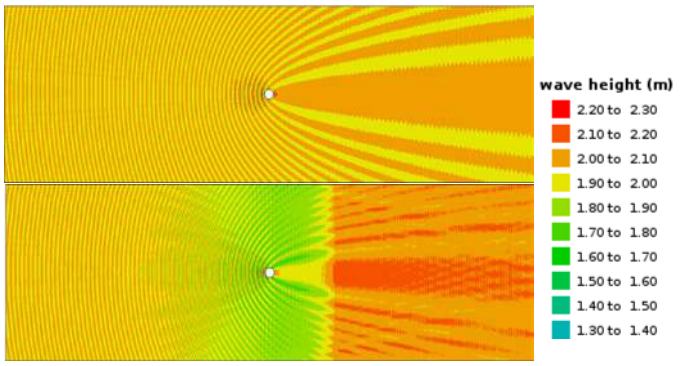

FIGURE 8: TOTAL WAVE HEIGHT WITHOUT (TOP) AND WITH (BOTTOM) THE VARIABLE BATHYMETRY

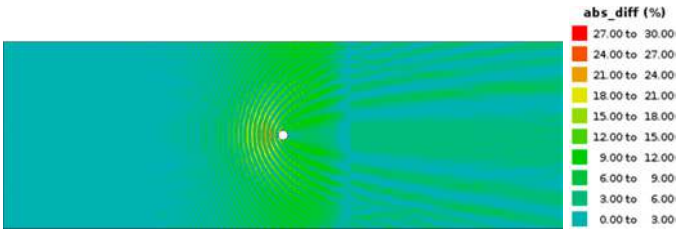

FIGURE 9: DIFFERENCE BETWEEN RESULTS IN FIG.8

We can see (fig 8 and 9) the importance of taking into account the variable bathymetry. There are two main differences, one before the body, and one above the top of the slope, but the main difference, given the same PTO on the WEC, is just in front of the body where the change in amplitude exceeds 25%. In the right part of the domain, the largest impact factor is the bathymetry.

3.3 Example with 11 WECs

With many WECs, simulations show that it is not necessary to compute beyond the second order of scattering (diffraction/radiation due to the first scattered waves), because the scattered wave height of one WEC on its nearest neighbour is lower than 1% after this. We study 11 WECs staggered configuration on three rows, and then compare the different results to show the impact of the bathymetry, as well as that due to the presence of the WEC array.

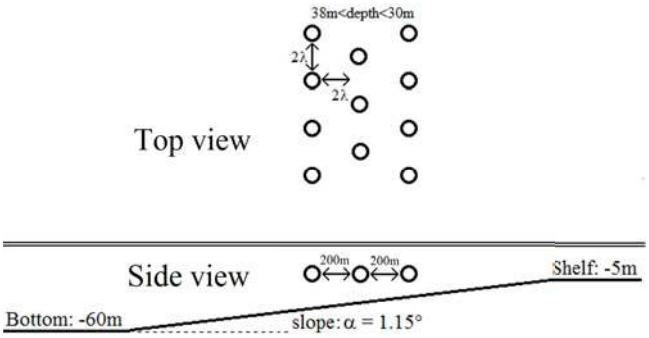

FIGURE 10: STAGGERED CONFIGURATION WITH 11 WECS

We choose a minimum depth of 30 m for the shallower area covered by the WEC array. Moreover, this depth corresponds to the typical depth for WEC farms.

3.3.1 Impact of the bathymetry on the incident wave First, we analyse the impact of the bathymetry on the incident wave height. The following result is obtained from the difference $(wave\_height_{variable\_bathy} - wave\_height_{flat\_bathy})$ (with a depth of 60 m for the flat bathymetry)

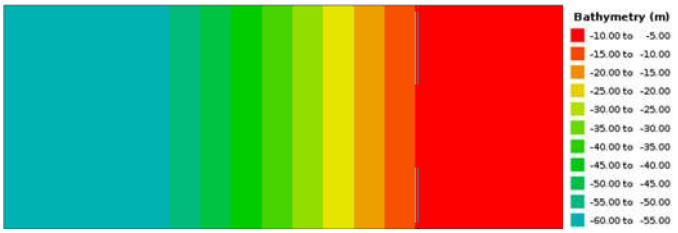

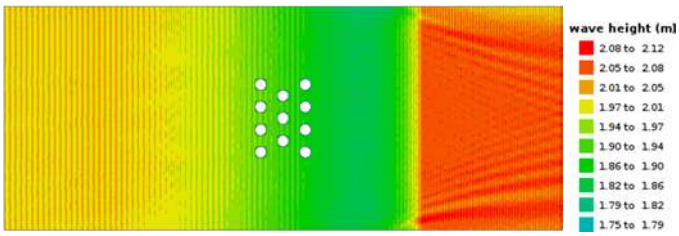

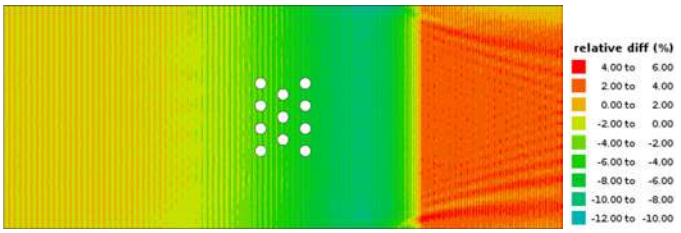

FIGURE 11: BATHYMETRY (TOP), INCIDENT WAVE HEIGHT WITH A SLOPE (MIDDLE) AND DIFFERENCE WITH THE INFINITE DEPTH CASE (BOTTOM)

Compared to the incident wave height which remains 2m with a flat bottom, we can see that the variable bathymetry has an important impact on the wave field. This varies from -25cm (-12.5%) in the shoaling zone to 10cm above the shelf (ie 5% with the formula $relative\_diff = \frac{(H_{var\_bathy} - H_{flat\_bathy})}{H_{flat\_bathy}}$).

3.3.2 Bathymetry impact on the scattered wave With the arbitrary PTO force imposed to the WECs, the heaving amplitude corresponds approximately to 50% of the incident wave height.
By summing the different scattered waves we obtain the following results. The bathymetry impact is obtained as the difference between the results, with a variable bathymetry and a flat bottom.

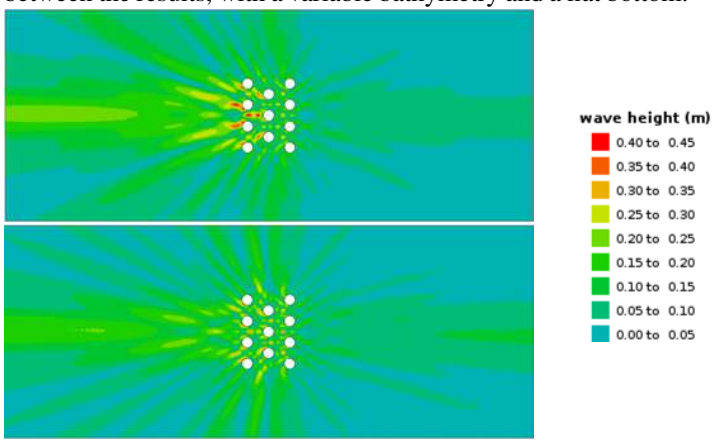

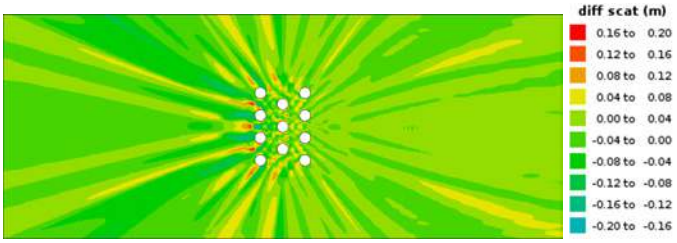

FIGURE 12: SCATTERED WAVE HEIGHT WITHOUT (TOP) AND WITH THE VARIABLE BATHYMETRY (MIDDLE) AND DIFFERENCE (BOTTOM)

As for the incident wave, the bathymetry affects the scattered waves. As it modifies wavelengths, potentials can be phase shifted and have a different direction compared to the case with a constant depth. That can explain why the difference between the two cases reaches 20cm (10% of the incident wave height) close to the WECs farm. Behind 3 wavelength, this difference decreases down to 6 cm because scattered waves are circular waves.

3.3.3 Bathymetry impact on the total wave field

Now, we compare the total wave height of the two cases with the same approach as in the previous paragraph. The total wave height under linear theory is obtained from:

$$H = \frac{2\omega}{g}.|\phi| \tag{10}$$

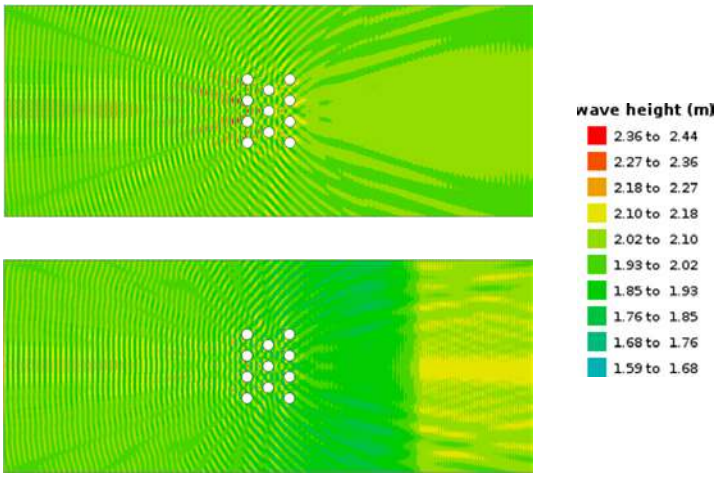

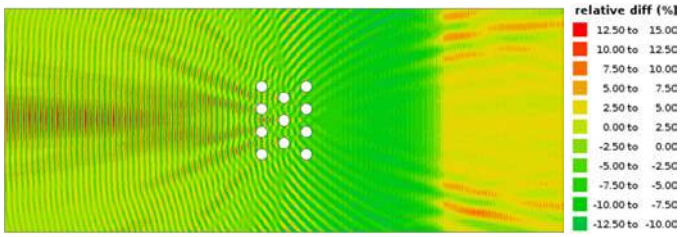

FIGURE 13: TOTAL WAVE HEIGHT WITHOUT (TOP) AND WITH THE VARIABLE BATHYMETRY (MIDDLE) AND DIFFERENCE (BOTTOM)

The difference rises up to 15% mainly due to the impact of the bathymetry on the scattered waves and to the shoaling process. This total difference is not the sum of the scattered and incident differences and can be lower than this sum due to the phaseing of the incident and scattered potentials.

3.4 WEC impact on the total wave field

Now, we focus on the impact of WECs on the total wave field with a flat bottom and a variable bathymetry. To do that, we subtract the incident potential to the total potential. We can get the relative difference:

$$relative\_diff = \frac{(H_{total} - H_{incident})}{H_{total}}$$

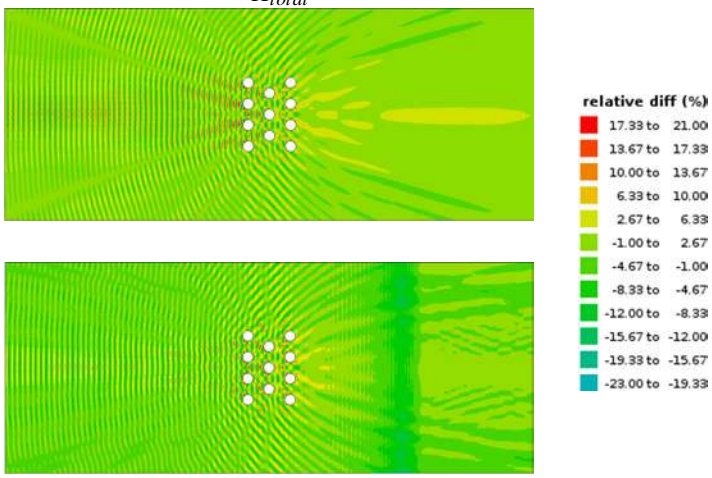

FIGURE 14: DIFFERENCE BETWEEN A DOMAIN WITH AND WITHOUT 11 WECS FOR A FLAT BOTTOM (TOP) AND A VARIABLE BATHYMETRY (BOTTOM)

As seen above, the height of the scattered waves of a WECs' farm reaches 25% of the incident wave height. The local impact of a farm is not negligible. This scattered wave height decrease as $\sqrt{\frac{1}{r}}$, therefore this impact is rapidly small.

In both cases, with a flat bottom and a variable bathymetry, the

magnitude of the difference is similar. However, on the upwave part of the farm, the impact of the farm is lower than with a flat bottom. This difference is probably due to the phase shift caused by the slope. The impact of the farm is significant over a 6 wavelength distance.
In the downwave part of the domain, the nearshore area, the difference is negative. It is due to the shoaling effect for the incident wave. This effect is negligible for the scatted waves.
The combined scattered waves of each WEC increase the impact, that is why we can see a large impact on figure 14.
Therefore, it is possible with this type of modeling to compare different configurations and choose the one that has a lower impact.

4 Conclusion/discussion

To look at the impact of a farm of WECs on a given area and to save time and maintain accuracy, we propose here a methodology coupling a diffraction/radiation code with a mild slope equation code, solving the wave propagation problem. This approach has the advantage to take into account an irregular bathymetry, which allows to deal with realistic domain. The cases under study with a variable bathymetry showed significant differences with flat bottom case. Taking this into account will allow us to optimize the organisation of farms and understanding their impact on the local wave field.
Our initial results look promising. We obtain reasonable computational time: the multi-bodies case with a variable bathymetry needs only one minute to compute the Kochin function, and less than two minutes for wave propagation. As we calculate the wave interactions up to the second order, we have 122 computations (but some are negligible) for 11 WECs. A point still to be looked at is the post-treatment, especially the interpolation of each WEC results, which needs more time because we have a mesh of around 20 millions elements.
Future application is to couple our results with a spectral model that includes a very large domain ($\sim$ 10km) with the coastline, which will allow to better understand the impact of a farm, combined with the coastline, on the wave field.

REFERENCES

[1] P.Troch, V.Stratigaki, T.Stallard, D.Forehand, M.Folley, J.P.Kofoed, M.Benoit, A.Babarit, Sanchez, D., Bosscher, L., P.Rauwoens, B.Elssser, P.Lamont-Kane, P.McCallum, C.McNatt, E.Angelelli, A.Percher, Moreno, E., S.Bellew, E.Dombre, F.Charrayre, M.Vantorre, J.Kirkegaard, and S.Carstensen, 2013. "Physical modelling of an array of 25 heaving wave energy converters to quantify variation of response and wave conditions". *10th European Wave and Tidal Energy Conference (EWTEC), Aalborg (Denmark)*, septembre.

[2] V.Twersky, 1952. "Multiple scattering of radiation by an arbitrary configuration of parallel cylinders". *Acoustical Society of America,* ***24***(1), january, pp. 42–46.

[3] M.Ohkusu, 1974. "Hydrodynamic forces on multiple cylinders in waves". *Symp.on Dynamics of Marine Vehicles and Structures in Waves, London*, pp. 107–112.

[4] B.H.Spring, and P.L.Monkmeyer, 1974. "Interaction of plane waves with vertical cylinders". *Coastal Engineering Proceedings, Copenhagen (Denmark)*, pp. 1828–1847.

[5] M.J.Simon, 1982. "Multiple scattering in arrays of axisymmetric wave-energy devices". *Journal of Fluid Mechanics,* ***120***, pp. 1–25.

[6] H.Kagemoto, and D.K.P.Yue, 1986. "Interactions among multple three-dimensional bodies in water waves: an exact algebraic method". *Journal of Fluid Mechanics,* ***166***, pp. 189–209.

[7] M.Folley, A.Babarit, B.Child, D.Forehand, L.O'Boyle, K.Silverthorne, J.Spinneken, V.Stratigaki, and P.Troch, 2012. "A review of numerical modelling of wave energy converter arrays". *In Proc. of the 31st International Offshore Mechanics and Artic Engineering (OMAE) Conference, Rio de Janeiro, Brazil.*

[8] A.Babarit, M.Folley, F.Charrayre, C.Peyrard, and M.Benoit, 2013. "On the modelling of wecs in wave models using far field coefficients". *In Proc. of the 10th European Wave and Tidal Energy Conference (EWTEC).*

[9] Wamit, user manual 7.0. http://www.wamit.com.

[10] G.Delhommeau, 1987. "Les problèmes de diffraction-radiation et de résistance de vagues: étude théorique et résolution numérique par la méthode des singularités (in french)". PhD thesis, école nationale supérieure de mécanique, Nantes (France).

[11] G.Delhommeau, 1993. "The seakeeping codes aquadyn and aquaplus". In Numerical Simulation of Hydrodynamics: Ships and Offshore Structures, Ecole Centrale Nantes.

[12] Opentelemac. http://www.opentelemac.org.

[13] J.C.W.Berkhoff, 1972. *Mathematical models for simple harmonic linear water waves.Wave diffraction and refraction*. Delft Hydraulics Lab Publication.

[14] P.G.Chamberlain, and D.Porter, 1995. "The modified mild-slope equation". *Journal of Fluid Mechanics,* ***291***, pp. 393–407.

[15] C.C.Mei, M.Stiassnie, and D.K.P.Yue, 2005. *Theory and application s of ocean surface waves; Part1: Linear aspects*. World Scientific, ch. Scattering by a vertical cylinder with circular cross section, pp. 364–368.

[16] J.Falnes, and K.Budal, 1982. "Wave-power absorption by parallel rows of interacting oscillating bodies". *Applied Ocean Research,* ***4***, pp. 194–207.

[17] B.Molin, 2002. *Hydrodynamique des structures offshore*. Technip, ch. les grands corps: theorie lineaire (in French), pp. 186–210.